Effect of High Pressure on Vibrational Modes of Polyiodides in Poly(vinyl alcohol) Films

Archita Sengupta,[†] Edward L. Quitevis,*[,†,‡] and Mark W. Holtz*[,‡]

Department of Chemistry and Biochemistry, and Department of Physics, Texas Tech University, Lubbock, Texas 79409

Received: September 4, 1997; In Final Form: October 13, 1997[⊗]

We have used resonance-Raman scattering to study the effects of hydrostatic pressure (to 80 kbar) on polyiodide chain vibrations in iodine-doped poly(vinyl alcohol) films. Two strong fundamental bands are observed along with overtone and combination bands. The low-energy band at 107 cm^{-1} is attributed to symmetric stretching of I_3^-. The higher lying band at 154 cm^{-1} is from symmetric stretching of the two end I_2 units in I_5^-. The I_3^- and I_5^- are intermixed within the polyiodide chains. The combination band arises from exciton coupling between molecules within the chains. Three primary effects are observed with increasing pressure. First, the Raman band at 107 cm^{-1} blue shifts under pressure, while the band at 154 cm^{-1} shifts weakly. This latter is attributed to the competing effects of compression, enhanced interaction of the outer I_2 with the central I^- (which weakens the outer I−I bond), and attractive host−guest interactions which increase in strength with compression. The second effect observed in the Raman bands is dramatically increasing line widths. This signifies locally nonhydrostatic conditions due to the variations in local microstructure within the polymer. Third, the *relative* intensities reverse in dominance as the pressure exceeds ≈18 kbar. We suggest that this is due to breaking of the I_5^- chain elements into I_2 and I_3^-, which is caused by the locally inhomogeneous strain conditions. The intensities reflect the changing populations in I_3^- and I_5^-. These three effects are also observed in the overtone and combination bands of the Raman spectra. High-pressure absorption measurements in the visible support our interpretation and confirm the important role played by attractive host−guest interactions.

I. Introduction

Poly(vinyl alcohol) (PVA) forms a dark blue complex with aqueous I_2 in the presence of KI.[1−14] The polyiodides in these complexes are believed to be quasi-one-dimensional. In thin film form, iodine-doped PVA is well-known as a high-quality optical polarizer.[2] The PVA−iodine complex has received much attention due to intense interest in how iodine is incorporated into the polymer host,[1,3,4,6,8,9,10] the nature of the interaction between the polyiodide chains and PVA,[5,6,9,10] and the structure of the polyiodides in the complex.[7,8,11−14] The optical properties of the PVA−iodine complex resemble those of the amylose−iodine or the starch−iodine complex[15,16] and other polymer−iodine complexes.[17,18] The structure and its relationship to the electronic and vibrational properties of these aggregates are not yet fully understood. Improving this understanding is the basic motivation for our experimental investigations.

Raman scattering is an important probe of structure because it is sensitive to both local and long-range order. It has been extensively used to resonantly probe the vibrational modes in several polyiodide compounds.[7,8,11−14,16,17a,18−21] In iodine-doped polymer systems, strong Raman bands between 100 and 200 cm^{-1}, and related overtone and combination scattering, have been identified as being due to various polyiodide species. However, controversy exists as to the structures of the polyiodide species giving rise to these bands.

Marks and co-workers[16b,c,f] performed comparative studies of amylose−iodine and several model polyiodide compounds. They concluded that the iodine in the amylose helix is predominantly in the form of linear I_5^-. Due to the similarities between the electronic absorption and resonance Raman (RR) spectra of amylose−iodine and those of PVA−iodine, the main dopant species in PVA−iodine probed by RR was thought to mainly be due to linear I_5^-. However, recent X-ray diffraction and Mössbauer studies[11,12] indicate that this may not be the only polyiodide species present in PVA films. In a previous study, we examined the low-temperature RR scattering from iodine-doped PVA films at 77 K and room temperature.[13,14] The low temperature data revealed several features that are not resolved at room temperature. We interpreted the results in terms of RR scattering mainly from chains of both I_3^- and I_5^-. Scattering enhancement was attributed to exciton states of I_3^--I_5^- dimers, in agreement with Mizuno et al.[21] In this article, we report new results from a high-pressure study that lend further support to this interpretation.

The fact that PVA films turn blue when soaked in aqueous I_2/KI solution and remain blue after the films are removed from solution strongly suggests that iodine, in the form of polyiodides, has a strong affinity for PVA. Recent electronic structure calculations show that isolated I_5^- is more stable in the bent C_{2V} form than in the linear $D_{\infty h}$ form.[22] It is clear though that in PVA films iodine binds to certain sites possessing local geometry and molecular properties that facilitate the formation of linear polyiodides. This would explain why linear polyiodides larger than I_3^- are only observed in the presence of host materials as in the case of iodine-doped PVA films,[7,8,11−14] the amylose−iodine complex,[16b,c,f] or iodinated-nylon-6.[17] X-ray diffraction and Mössbauer studies of stretched iodine-doped PVA films show that the polyiodide chains are oriented along the stretch direction.[11,12] Furthermore, there is an enhancement of the PVA−iodine complex as evidenced by the characteristic UV−vis band at 600 nm when PVA films are stretched while in an aqueous I_2/KI solution.[10a]

Commercially available PVA is atactic and should therefore

* To whom correspondence should be addressed.
† Department of Chemistry and Biochemistry.
‡ Department of Physics.
⊗ Abstract published in *Advance ACS Abstracts,* December 1, 1997.

S1089-5647(97)02898-8 CCC: $14.00

be amorphous in the bulk state.[23] However, X-ray diffraction reveals regions of microcrystallinity implying that bulk PVA is semicrystalline as opposed to being purely amorphous.[3] Interestingly, X-ray diffraction patterns indicate that in iodine-doped PVA films, fabricated by soaking in low concentrated I_2/KI solutions ($[I_2] < 0.002$ M), such as the films used in our studies, polyiodides are localized in the amorphous regions.[3,10e] On the simplest level, the "spaghetti" model[23] for amorphous polymers can be invoked to explain the PVA−iodine data. In this model, the PVA chains in the amorphous region weave in and out among each other as in a bowl of spaghetti. Examination of adjacent polymer chains reveals local order with the chains appearing to lie more or less parallel to each other, as would be the case in a stretched PVA film. One could envision polyiodide chains incorporated between PVA chains in randomly oriented domains of local order and parallel geometry. The parallel geometry would explain why linear I_5^-, rather than the bent form, is found in PVA−iodine. On the basis of Mössbauer and X-ray data[11,12] the polyiodide chains contain varying amounts of I_3^- and I_5^- anions. These include chains of the form $(I_3^-)_n$ and $(I_5^-)_m$, analogous to homopolymers, and chains of form $(I_3^-)_l(I_5^-)_k$, analogous to random or block copolymers.

To our knowledge, high hydrostatic pressure has not been used to examine the RR scattering in these systems. The effects of hydrostatic pressure are very complex in polymers.[24] Linear polymers are pressure-sensitive materials due to their weak interchain interactions. The initial effect of compression will primarily be to quench any voids present within the polymer film. This will contribute to distortion of the polymer chains, with increasing pressure, due to medium-range nonuniformity within the polymer film. If the description given above is correct, regarding the manner in which polyiodides are distributed within iodine-doped PVA films, then the effect of pressure on the polyiodide chains present in iodine-doped PVA films will likewise be complex. We expect these will be kinked on the macroscopic (chain length) scale. On the microscopic scale, the I_3^- and I_5^- chain elements will be compressed. Pressure-induced vibrational frequency shifts in these polyiodide species will depend on the nature of the chemical bonding, mechanical anharmonicities, and interactions within the PVA host. Compression (bond-length shortening) is typical in high-pressure experiments, while kinking (resulting in diminished long-range order) is not. Additionally, strong attractive dipole−induced dipole interactions between the highly polarizable guest polyiodide species and polar PVA host should influence the vibrational and electronic levels. Compression will increase the relative strength of these interactions because of their $1/r^6$ dependence.[25] All of these effects have implications for the vibrational modes in RR scattering and serve as motivation for the results we report.

The remainder of this article is organized as follows. In section II we discuss briefly the samples and experimental setups. Following this, in section III we present the results of our high-pressure RR study together with a discussion of the observations. In section IV, we present our measurements of the PVA−iodine complex visible absorption band under pressure. Finally, in section V, we summarize our results.

II. Experimental Methods

Iodine-doped PVA films were prepared by the method described previously.[13,14] Thicknesses varied between 20 and 100 μm. Films were characterized by UV−visible absorption spectroscopy. A broad band centered near 595 nm is attributed to the PVA−iodine complex. Bands were also present at 191 and 211 nm and at 296 and 361 nm. The former are due to I^- and the latter are due to I_3^-, based on comparison with the absorption spectrum of an aqueous I_2/KI solution.

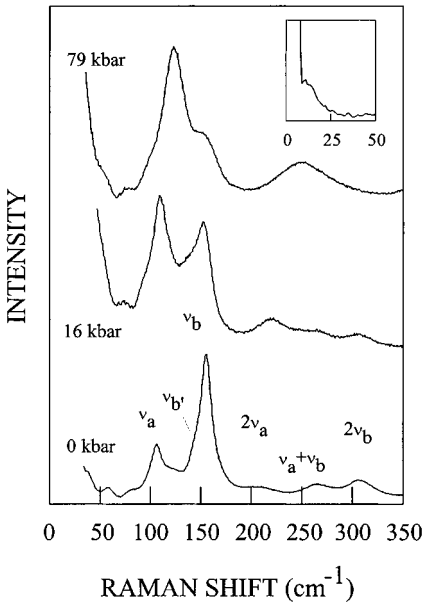

Figure 1. Room-temperature Raman spectra of PVA−iodine taken at three pressures (λ_L = 647.1 nm). Clearly seen are the shifting, broadening, and changes in relative intensities described in the text. The inset shows the low-wavenumber spectrum (λ_L = 514.5 nm), revealing one band near 12 cm^{-1}.

The Raman measurements were carried out using 647.1 nm light from a krypton-ion laser. A micro-Raman instrument focused the light onto the sample with a spot size <10 μm in diameter and incident laser power ≈10 mW at the sample. This was found to be well below the power needed to blister a free-standing sample. Backscattered light was collected, collimated, and then passed through a holographic notch filter to attenuate the laser Rayleigh scattering. The remaining light was focused through the entrance slit of a 0.5 m single monochromator, and the spectrum was measured by a charge-coupled device detector. This was controlled by a data acquisition system and a personal computer. With this system, Raman spectra with resolution better than 2 cm^{-1} and spanning a 500 cm^{-1} range were obtained with a typical collection time of 60 s. For examining very low vibrational energies, a triple-additive-dispersive Raman system was used with 514.5 nm argon-laser excitation.[26]

Hydrostatic pressures to 80 kbar were generated using a diamond-anvil cell (DAC). All measurements were done at room temperature. A stainless steel gasket was employed, with a 4:1 mixture of methanol and ethanol for transmitting the pressure and ruby for pressure calibration.[27] Ruby fluorescence was excited using an argon-ion laser (514.5 nm). Final corrections to the actual pressures were made by measuring the ruby fluorescence at 1 atm (i.e., with a bubble present) following each pressure series.

The absorbance was also measured under hydrostatic pressure using a Shimadzu UV2101 spectrometer. The weak throughput of the DAC made it necessary to decrease the intensity of the reference beam using a pinhole aperture. Due to the optical properties of the DAC, we were able to study only the visible range of the absorbance spectrum. Beyond 50 kbar, the absorbance was too weak to measure. Therefore, we restrict our attention to the 0−50 kbar range.

III. Effect of Pressure on the Iodine Raman Bands

A. Pressure Shifts. Figure 1 shows the Raman spectra for the 3.9 mM iodine doped PVA film at ambient pressure (P =

TABLE 1: Zero-Pressure Vibrational Energies and Their Pressure Dependences for the Primary Raman Bands[a]

mode designation	ν_0 (cm^{-1})	$\partial\nu/\partial P$ (cm^{-1}/kbar)
ν_a	107.0 ± 0.6	0.22 ± 0.01
ν_b'	139.9 ± 1.4	0.08 ± 0.03
ν_b	154.4 ± 0.8	0.04 ± 0.02
$2\nu_a$	212.1 ± 1.0	0.49 ± 0.03
$\nu_a+\nu_b$	265.0 ± 1.5	0.26 ± 0.06
$2\nu_b$	307.0 ± 0.7	0.15 ± 0.04

[a] Results are from linear least-squares fits to the data (Figure 3).

0), and at 16 and 79 kbar. At $P = 0$, the dominant features are denoted $\nu_a = 107$ cm^{-1} and $\nu_b = 154$ cm^{-1}, corresponding to Raman scattering from fundamental vibrational modes of the polyiodide chains. These are attributed to Raman-active vibrations from two separate species comprising a given polyiodide chain. The band at ν_a stems from I_3^- elements in the polyiodide chains, while the band at ν_b is attributed to the I_5^- elements. Our results agree with recent electronic structure calculations to the extent that these two bands arise from two different polyiodide species.[22] However, our results differ from the calculations, in that the calculations imply that ν_b arises from bent as opposed to linear pentaiodide. In addition, weaker bands are clearly observed in Figure 1 at 212, 307, and 265 cm^{-1}. These are respectively identified as overtones ($2\nu_a$ and $2\nu_b$) and a combination band ($\nu_a + \nu_b$). Peak positions, together with assignments and pressure shift rates, are listed in Table 1. A slight asymmetry is also seen on the low wavenumber shift side of ν_b, denoted ν_b'. This was clearly resolved at low temperatures and was tentatively assigned to the Raman-active stretching of the outer I−I of bent I_5^-.[14]

The inset to Figure 1 shows the Raman spectrum in the low vibrational energy range. One band is reproducible near 12 ± 1 cm^{-1}. Recent calculations suggest that this is from an A_1 symmetry bending mode of the bent I_5^-.[22] Due to its proximity with the laser line, we were not able to study the effect of pressure on the 12 cm^{-1} band.

The presence of combination bands, at first glance, would seem to contradict the assignment of the ν_a and ν_b bands in the RR spectrum to two separate polyiodide species. Mizuno et al.,[21] however, proposed that the combination bands arise from a resonance effect involving an excited state formed by the excitonic interactions between I_3^- and I_5^- species. This is analogous to the excitonic interactions between molecules in H- or J-aggregates of cyanine dyes.

In the exciton model[14] for a dimer consisting of two different molecules, the electronic ground state for the molecular dimer is given by the product state $|g,g\rangle = |g\rangle_1|g\rangle_2$, where $|g\rangle_1$ and $|g\rangle_2$ represent the electronic ground states for molecules 1 and 2, separately. We define localized electronic excited states for molecules 1 and 2, $|g,e\rangle = |g\rangle_1|e\rangle_2$ and $|e,g\rangle = |e\rangle_1|g\rangle_2$. These correspond, respectively, to a situation in which molecule 1 is unexcited and 2 is excited, and vice versa, with transition frequencies given by ω_1 and ω_2. As a result of dipolar coupling, in-phase (+) and out-of-phase (−) exciton states given by $|\pm\rangle = (1/2)^{1/2}(|e,g\rangle \pm |g,e\rangle)$ are generated. The difference in the energy of these two states is given by 2ϵ, where ϵ is called the exciton displacement. For linear polyiodide chains, the head-to-tail arrangement will be assumed. For this configuration, $|+\rangle$ is lower in energy then $|-\rangle$ and carries most of the oscillator strength. The exciton displacement ϵ arises from the delocalization of excitation between molecules 1 and 2. Its value is determined by the transition moments of the individual molecules and their separation. The center line of the exciton splitting is given by $[(\omega_1 + \omega_2)/2] + \Delta D$. The term ΔD is equal to the difference of the interaction energy of the charge distributions of the excited state of one molecule, with the ground state of the other molecule and that of the charge distributions with both molecules in the ground state. The frequency for the $|g,g\rangle \rightarrow |+\rangle$ transition is given by $\omega_+ = [(\omega_1 + \omega_2)/2] + \Delta D - \epsilon$. Figure 2 illustrates the mechanism by which RR scattering gives rise to a combination band. This picture assumes one vibrational mode for each molecule. The notation (υ_1,υ_2) denotes the vibrational state of the dimer. For example, (1,2) would correspond to one quantum of vibrational excitation in molecule 1 and two quanta of vibrational excitation in molecule 2. Figure 2 depicts a photon incident at frequency $\omega_{ex} \approx \omega_+$ and a photon scattered at frequency ω_s, with the energy difference $\hbar(\omega_{ex} - \omega_s)$ equal to the level separation between the ground vibrational state (0,0) and the combination state (1,1) of a mixed dimer in the electronic ground state. This diagram describes the mechanism for the Raman scattering that gives rise to the combination band $\nu_a + \nu_b$ for an $I_3^- - I_5^-$ dimer. The combination band at $\nu_a + 2\nu_b$ can also be rationalized by this exciton model.

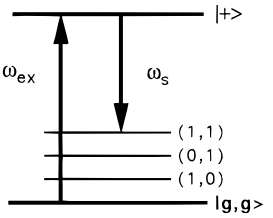

Figure 2. Energy level diagram illustrating the mechanism for RR scattering by a combination band with enhancement from the $|+\rangle$ exciton state of a $I_3^- - I_5^-$ dimer.

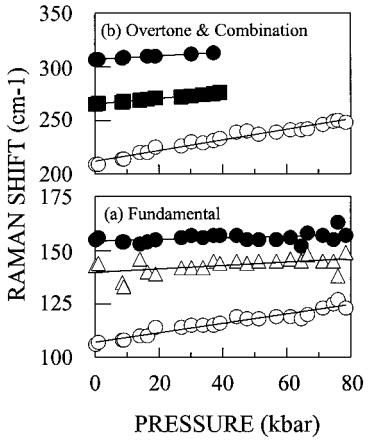

Figure 3. Peak position vs pressure data summaries for the polyiodide related first (a) and second (b) order Raman bands seen in Figure 1. Open (closed) circles are for features ν_a (ν_b), with the same symbols for overtones of these modes. Filled squares are for the $\nu_a + \nu_b$ combination. Open triangles are for the ν_b' band. Zero-pressure peak positions and linear pressure coefficients are listed in Table 1.

Because electronic transitions for I_3^- occur at wavelengths that are shorter than the excitation wavelengths used in this study, one should not expect resonance enhancement to occur for the Raman bands of I_3^-. However, exciton-coupling generates excited states that lie at energies lower than those of I_3^-, and therefore resonance enhancement can occur at these longer excitation wavelengths. This provides an explanation for the strong fundamental band and overtone bands with significant intensity for I_3^-.

As pressure is applied several consequences for the Raman bands are observed. We first discuss the Raman frequencies. Peak positions, from fits to the spectra, vs pressure are shown in Figure 3. The dependences are linear, with the results of least-squares fits given in Table 1. First, ν_a increases at a rate

of 0.22 ± 0.01 cm^{-1}/kbar. Increasing vibrational energy is characteristic upon compression by external pressure. For comparison, we examine the *relative* pressure rate, $(1/\nu_0)(\partial\nu/\partial P)_0$, rather than the absolute shift. For ν_a this is $(2.1 \pm 0.1) \times 10^{-3}$ $kbar^{-1}$, which is in surprisingly close agreement with high-pressure measurements of I_2 in organic solvents.[28] Differences are expected because the vibrational frequency shifts are sensitive to the molecular size of the solvent and solute species and the strength of the attractive, long-range, solvent−solute interactions.[28] Both factors differ in the present case from I_2 in organic solvents, resulting in subtle variations in the iodine-vibration pressure coefficients within the respective hosts. The comparison is made here simply because it establishes order of magnitude consistency in the effects of external pressure on the vibrations of I_3^- in iodine−PVA and I_2 in organic solvents.

In sharp contrast, ν_b shifts very weakly with pressure. This mode is attributed to the outer I−I symmetric stretch of linear I_5^-. Essentially, ν_b is associated with the vibrational frequency of the outer I_2 units. Pressure is expected to increase the interatomic interaction by molecular compression, which typically raises the vibrational frequency. However, this alone fails to explain the observed weak pressure coefficient observed. The bonding in linear I_5^- can be understood in terms of donor−acceptor interactions between I_2 and I^-.[29] On the basis of simple molecular orbital arguments, σ donation can occur from electron pairs on I^- to σ antibonding orbitals on either of the outer I_2 units, which weakens the I_2 bond and lowers the I_2 vibrational frequency. Pressure increases the interaction between the central donor I^- and its two nearest I_2 acceptors. This in turn leads to a reduction in the bond strength of the outer I−I bonds and a concomitant decrease in the outer I_2 force constant. This interplay between opposing effects has previously been seen in the high-pressure Raman data for metal carbonyl compounds[30,31] and conducting polymers.[32] Furthermore, attractive host−guest interactions will act to reduce the pressure coefficients.[28] The importance of these interactions is confirmed by the absorbance measurements in section IV. The net result is several competing effects, the combination of which produces the small pressure coefficient observed for ν_b.

The ν_b' band at 140 cm^{-1} was obtainable from the room-temperature spectra only by fitting the spectra over the fundamental ranges. A consistent pressure dependence was found in the line width (which increased with pressure). However, the most convincing evidence is exhibited in the pressure dependence of the frequency of this band, as seen in Figure 3a. It is seen that this band follows ν_b, although its pressure coefficient is slightly higher (Table 1).

In the Raman scattering from the overtone and combination bands, the pressure shifts should be approximately equal to the sum of the pressure coefficients of the parent fundamental bands. As is seen in Table 1, the $2\nu_a$ band shifts at a rate only slightly higher than twice the rate at which ν_a shifts. Combination $\nu_a + \nu_b$ shifts at a rate equal to the sum of the two pressure coefficients for the parent bands. This is very convincing evidence that the combination assignment is correct. Overtone $2\nu_b$ shifts significantly faster than twice the rate of ν_b but is within the total error. In view of the breadth of these second-order lines, it is difficult to pinpoint the peak position. Furthermore, for the limited pressure range over which ν_b and especially $2\nu_b$ are measured, we do not consider the discrepancy to be of consequence. We would like to point out, however, that there is the possibility that the overlap of a neighboring, unresolved band could distort the line shape to the extent that the peak position is affected as the pressure rises. This would cause the pressure coefficient of the overtone band to be slightly inflated beyond that expected from an isolated band.

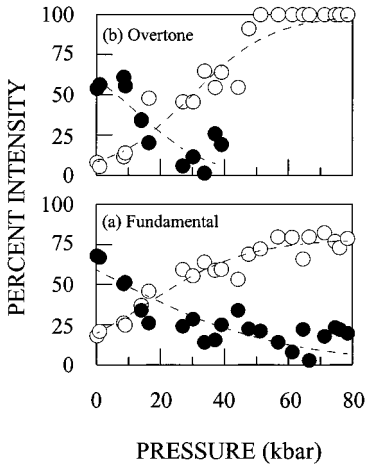

Figure 4. Dependence of relative intensities on pressure for the ν_a and ν_b bands in first order and their respective overtones. Symbols are the same as in Figure 3. These were obtained from fits to the data taking into account only those Raman bands in either (a) or (b). For both sets of features, crossover in dominant intensity occurs near 18 kbar. The dashed curves are guides for the eye.

B. Raman Line Widths. What is also evident in Figure 1 is that pressure significantly broadens the polyiodide Raman lines in the PVA−iodine complex. This was best tracked in ν_a and ν_b, using fits to the spectra. We find that the ν_a line width increases from the zero-pressure value ($\Delta\nu_a = 13$ cm^{-1}) at a rate of 0.18 ± 0.04 cm^{-1}/kbar. The line width of ν_b is slightly larger at $P = 0$ ($\Delta\nu_b = 15$ cm^{-1}) and increases at a rate of 0.22 ± 0.06 cm^{-1}/kbar. Over the pressure range that we could reliably determine the line widths, the overtone bands were approximately twice as broad as their parent first-order lines. We interpret the pressure-induced broadening as evidence for *locally* nonhydrostatic conditions affecting the iodine chains. These conditions are inevitable with a nonhomogeneous medium and can manifest themselves through increasingly bent and broken chain distortions. Both manifestations lead to reduced long-range order and, in the case of broken structures, a shift in the molecular populations of the chain elements.

C. Intensities. A very interesting observation from the pressure data is the shift in relative intensities evident in Figure 1. As pressure increases, the ν_a band rapidly gains intensity while the ν_b band weakens. This is summarized in Figure 4a, which shows the percent intensity of these two first-order Raman bands. These were obtained from fits to the spectra at each pressure and normalized to the sum intensities of these two bands only. The dashed lines are fits to the data using sigmoidal and inverse-sigmoidal functions. These curves are included in Figure 4 only as guides to the eye. The rise in intensity for the ν_a band, with decreasing ν_b intensity, is also evident in the overtone features (similarly calculated) in Figure 4b. Both the fundamental and overtone Raman band intensity profiles show a crossover in dominant line intensity near a pressure of 18 kbar.

We interpret the shift in relative intensities summarized in Figure 4 in the following manner. The ν_a band stems from molecular vibrations of I_3^- elements, and the ν_b band is from vibrations of I_5^- elements within the mixed polyiodide chains. Our Raman data suggest that compression increases the I_3^- population at the expense of I_5^- within the polyiodide chains. The simplest explanation is that this is accomplished by breaking of the I_5^- chain elements into I_3^- and I_2. This proposition is consistent with the preceding discussion of the broadening seen in the Raman bands with increasing pressure.

Our low-temperature Raman study[14] revealed the presence of Raman scattering by I_2 at 219 cm^{-1} (ambient pressure). If pressure increases the I_2 population, a natural question to ask is whether one should see Raman scattering from I_2. However, it was necessary to measure this spectrum at 77 K in order to clearly observe the I_2 band. At room temperature, it is merged with the $2\nu_a$ overtone. Since the I_2 Raman band is expected to shift at approximately the same absolute rate as our $2\nu_a$ band,[28] it is impossible for us to resolve the two lines in our room-temperature, high-pressure measurements. Therefore, we cannot eliminate the possibility that some of the intensity enhancement and broadening of $2\nu_a$ in Figure 1 is due to the presence of an overlapping I_2 Raman band.

Within our picture, the increasing I_3^- population, at the expense of I_5^-, would be a consequence of the chain folding and diminishing long-range order within the polyiodide chains, discussed in relation to the line widths (section III.B). I_5^- elements are still present to pressures of 80 kbar, as the ν_b band is still clearly observed, permitting exciton coupling between the different chain elements. The intensity pattern observed is difficult to interpret within the model that the ν_a and ν_b bands both stem from vibrations of an I_5^- chain element. If this were the case, we would expect a similar dependence of the band intensities on pressure, in contrast to what is observed.

We mention here that the measured *absolute* intensities of the fundamental bands (which were both obtained up to our maximum pressure of 80 kbar) exhibited trends in the low-pressure range similar to what we discussed in connection with the *relative* intensities. That is, the ν_a intensity increases with pressure while the ν_b band decreases in strength. However, both measured intensities remained strong over the entire pressure range studied. This may indicate that the resonance conditions are changing, but we are not pressure tuning beyond RR conditions. Visually, the film becomes less opaque in the visible with increasing pressure. This is consistent with two possible effects. First, the 595 nm absorption band may be shifting out of the visible with pressure. Second, the absorption may be weakening with pressure. This latter effect would be expected if the I_5^- population is diminishing with pressure.

IV. Absorption Properties

To test if pressure tunes the visible absorption out of resonance conditions with the 647.1 nm laser excitation, we measured the absorbance spectrum at several pressures. Figure 5 shows the effect of pressure on the absorption band near 600 nm. As pressure increases, the band red shifts and weakens. This is in agreement with what is observed visually: the film becomes less opaque with increasing pressure. Most relevant to our Raman investigation is the observation that the 647.1 nm Raman excitation remains well within the absorbance band. This indicates that the absorption band is not pressure shifting beyond resonance conditions. The weakening of the absorbance is consistent with the interpretation of our Raman data. Namely, the I_5^- population is diminishing with pressure, and the evolving polyiodide chain structures remains in resonance with the Raman excitation.

We also notice that the absorption band in Figure 5 further broadens under pressure. At ambient pressure the absorption band is approximately 160 nm broad. This grows approximately linearly to 280 nm at 50 kbar. We expect the nonuniform environment of the polyiodide to become more varied with compression of the polymer host. The increasing line width is consistent with our expectation that the nonuniform environment of the polyiodide chains becomes more varied with compression of the polymer. This conclusion was also reached from our Raman data. Increased nonuniformity will result in a broader distribution of polyiodide structures, causing the optical transitions to further broaden.

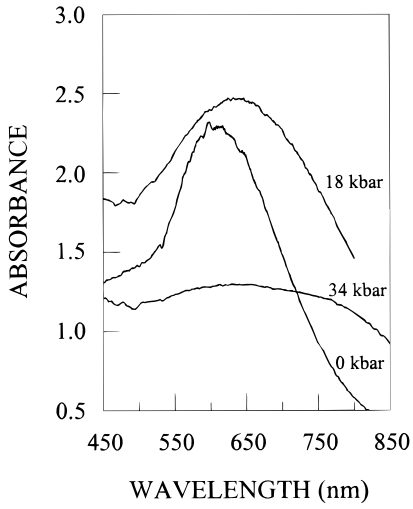

Figure 5. Absorbance spectra at three pressures. The red-shifting, broadening, and weakening of the visible polyiodide absorption are described in the text.

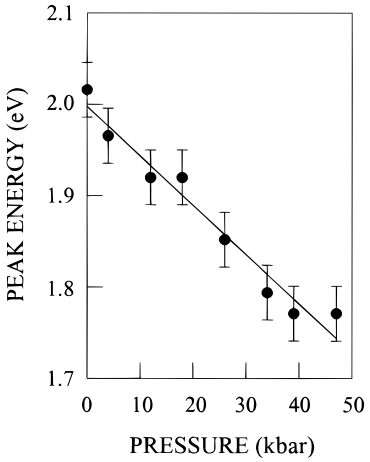

Figure 6. Pressure shift of the absorbance peak position from spectra as in Figure 5. The red shift is consistent with attractive guest−host interactions.

In Figure 6 we summarize the effect that pressure has on the peak position of the visible absorption band. The absorption band red shifts under pressure according to

$$\hbar\omega = \hbar\omega_0 + \alpha P \qquad (1)$$

where $\hbar\omega_0 = 1.998 \pm 0.010$ eV and $\alpha = -5.4 \pm 0.4$ meV/kbar from a least-squares linear fit to the data. Drickamer has reviewed the effects of pressure on electronic transitions for a range of solvent−solute interaction strengths.[33] In highly polarizable systems, for which attractive host−guest forces are present, these interactions contribute to red-shifting upon compression. In particular, our results for α in eq 1 are comparable to what is observed for the highly polarizable tetracyanoquinodimethane (TCNQ) crystals or TCNQ dissolved in several polymers.[33] This comparison is quite reasonable, given that polyiodides have been touted as being a type of quasi-unidimensional molecular system.[16c] It is therefore reasonable, given the highly polarizable polyiodide and the polar nature of PVA, that attractive intermolecular interactions play an important role in the effects of pressure on the iodine−PVA system.

In the amorphous region of the polymer, hydroxyl groups along the PVA chains will interact with the polyiodide species

via dipole−induced dipole forces. This appears to be necessary for complex formation to occur. In one of the models for amylose−iodine complex, dipole−induced dipole interactions between the net dipole moment along the axis of the amylose helix and the polarizable iodine atoms within the helix help to stabilize the complex.[15g] It is also reasonable to assume that at high-pressure some of these regions of parallel geometry will collapse, causing I_5^- to fold or break up into I_2 and I_3^- subunits. This would explain the increase in the intensity of the ν_a band due to I_3^- and the decrease in the intensity of the ν_b band due to I_5^-. The pressure-induced shift of the absorption band is also consistent with the guest−host interaction that we perceive to be occurring between the polyiodide species and PVA. This type of polymer conformational change under hydrostatic pressure has already been studied in regard to the conjugation breaking in polydiacetylene.[32]

Clearly, not all of the I_5^- breaks up, as evidenced by the persistence of the ν_b Raman band. This would suggest that some of the binding sites remain intact even under pressure. However, because of the amorphous nature of these binding sites, the application of pressure causes the sites to distort and therefore the interaction energy between the polymer host and I_5^- to change. The broadening of both the electronic absorption and vibrational bands is consistent with the inhomogeneous nature of these sites. Note that the short-range, $1/r^6$ dependence of the dipole−induced dipole attraction is also consistent with the strong affinity between iodine and PVA.

V. Summary

We have used high-pressure RR spectroscopy to study the polyiodide chains in iodine-doped PVA films. Several interesting features are observed in the data (see Figure 1).

Each Raman band shifts under pressure but at substantially different rates. The 107 cm^{-1} band shifts fairly rapidly with pressure (Figure 3). This band is attributed to Raman active stretching of the I_3^- chain elements within the intermixed I_3^- and I_5^- iodide chains. The 154 cm^{-1} band shifts very weakly. This band is attributed to I_5^- elements within the same chains. The weak shift is attributed to the combined effects of compression and subsequent enhancement of donor−acceptor interactions between the central I^- and the two outer I_2 in I_5^-. Additionally, attractive electrostatic interactions between the polyiodide and PVA molecules will diminish the vibrational energies. We observe basic agreement between the fundamental, overtone, and combination features in the RR spectra under pressure. This supports the exciton-coupling model for the interaction between the molecules within the polyiodide chains.

Pressure broadens the observed Raman lines. This is attributed to distortion of the iodine chains, which differs significantly from simple compression. Such distortion is expected for polyiodide chains in the highly inhomogeneous PVA host.

We observe that the *relative* intensities of the bands from I_3^- and I_5^- ionic molecules reverse roles under pressure (Figure 4). That is, the I_5^- diminishes in intensity, while the I_3^- band increases. Similar effects are seen in the second-order spectrum. A crossover pressure of 18 kbar is found. This third effect is attributed to pressure-induced breaking of the I_5^- chain elements into I_3^- and I_2. Such a reversal in intensities is interpreted naturally within the mixed-chain elements picture,[14] but not within the picture of single molecular elements comprising the iodine chains.

The optical absorbance in the visible was studied under hydrostatic pressure (Figure 5). We observed that the absorption band associated with the iodine−PVA complex diminishes in strength and broadens with pressure. In addition, the band red-shifts with increasing pressure. The weakened absorbance and broadening are consistent with our picture of a diminishing I_5^- population due to compression and locally nonhydrostatic conditions. The red-shift implies that pressure enhances attractive guest−host interactions due, primarily, to the high polarizability of iodine and the dipolar character of PVA.

Acknowledgment. The donors of the Petroleum Research Fund, administered by the American Chemical Society, are gratefully acknowledged for partial support of this research (M.H.). This research was partially supported by the Robert A. Welch Foundation (D-1019) to E.L.Q. We thank G. Gellene for sharing a preprint of ref 22.

References and Notes

(1) (a) West, C. D. *J. Chem. Phys.* **1947**, *15*, 689. (b) West, C. D. *J. Chem. Phys.* **1949**, *17* 219.
(2) Land, E. H. *J. Opt. Soc. Am.* **1951**, *41*, 957.
(3) Haisa, M.; Itami, H. *J. Phys. Chem.* **1957**, *61*, 817.
(4) Imai, K.; Matsumoto, M. *J. Polym. Sci.* **1961**, *55*, 335.
(5) Telebev, L. G.; Mikulskii, G. F.; Korchagina, E. P.; Glikman, S. A. *Vysokomol. Soedin.* **1965**, *7*, 123.
(6) (a) Zwick, M. M. *J. Appl. Polym. Sci.* **1965**, *9*, 2393. (b) Zwick, M. M. *J. Polym. Sci. A-1* **1966**, *4*, 1642.
(7) (a) Inagaki, F.; Harada, I.; Shimanouchi, T.; Tasumi, M. *Bull. Chem. Soc. Jpn.* **1972**, *45*, 3384. (b) Inagaki, F.; Harada, I.; Shimanouchi, T.; Tasumi, M. In *Advances in Raman Spectroscopy, Proceedings of the Third International Conference on Raman Spectroscopy;* Mathieu, J. P., Ed.; Hayden & Sons: New York, 1973; Vol. 1, pp 370−378.
(8) Hayashi, S.; Hirai, T.; Hojo, N.; Sugeta, H.; Kyogoku, Y. *J. Polym. Sci. Polym. Lett. Ed.* **1982**, *20*, 69.
(9) (a) Yokota, T.; Kimura, Y. *Makromol. Chem.* **1984**, *185*, 749. (b) Yokota, T.; Kimura, Y. *Makromol. Chem.* **1985**, *186*, 549. (c) Yokota, T.; Kimura, Y. *Makromol. Chem. Rapid Commun.* **1986**, *7*, 249. (d) Yokota, T.; Kimura, Y. *Makromol. Chem.* **1990**, *190*, 939.
(10) (a) Oishi, Y.; Miyasaka, K. *Polym. J.* **1986**, *18*, 307. (b) Oishi, Y.; Miyasaka, K. *Polym. J.* **1987**, *19*, 331. (c) Oishi, Y.; Yamamoto, H.; Miyasaka, K. *Polym. J.* **1987**, *19*, 1261. (d) Choi, Y.-S.; Oishi, Y.; Miyasaka, K. *Polym. J.* **1990**, *22*, 601. (e) Sakuramachi, H.; Choi, Y.-S.; Miyasaka, K. *Polym. J.* **1990**, *22* 638.
(11) Seto, M.; Maeda, Y.; Matsuyama, T.; Yamaoka, H.; Sakai, H. *Hyperfine Interact.* **1991**, *68*, 221.
(12) Yokoyama, T.; Kaneyuki, K.; Sato, H.; Hamamatsu, H.; Ohta, T. *Bull. Chem. Soc. Jpn.* **1995**, *68*, 469.
(13) Sengupta, A. M.S. Thesis, Texas Tech University, 1996.
(14) Sengupta, A.; Holtz, M.; Quitevis, E. L. *Chem. Phys. Lett.* **1996**, *263*, 25.
(15) (a) Rundle, R. E.; Edwards, F. C. *J. Am. Chem. Soc.* **1943**, *65*, 554. (b) Rundle, R. E.; French, D. *J. Am. Chem. Soc.* **1943**, *65*, 558. (c) Rundle, R. E.; French, D. *J. Am. Chem. Soc.* **1943**, *65*, 1707. (d) Rundle, R. E.; Edwards, F. C. *J. Am. Chem. Soc.* **1943**, *65*, 2200. (e) Baldwin, R. P.; Bear, R. S.; Rundle, R. E. *J. Am. Chem. Soc.* **1944**, *66*, 111. (f) Rundle, R. E.; Foster, J. F.; Baldwin, R. R. *J. Am. Chem. Soc.* **1944**, *66*, 2116. (g) Stein, R. S.; Rundle, R. E. *J. Chem. Phys.* **1948**, *16*, 195.
(16) (a) Marks, T. J.; Webster, D. F.; Ruby, S. L.; Schultz, S. J. *J. Chem. Soc. Chem. Commun.* **1976**, 444. (b) Teitelbaum, R. C.; Ruby, S. L.; Marks, T. J. *J. Am. Chem. Soc.* **1978**, *100*, 3215. (c) Marks, T. J. *Ann. N. Y. Acad. Sci.* **1978**, *313*, 594. (d) Cowie, M.; Gleizes, A.; Grynkewich, G. W.; Kalina, D. W.; McClure, M. S.; Scaringe, R. P.; Teitelbaum, R. C.; Ruby, S. L.; Ibers, J. A.; Kannewurf, C. R.; Marks, T. J. *J. Am. Chem. Soc.* **1979**, *101*, 2921. (e) Teitelbaum, R. C.; Ruby, S. L.; Ibers, J. A.; Kannewurf, C. R.; Marks, T. J. *J. Am. Chem. Soc.* **1979**, *101*, 2921. (f) Teitelbaum, R. C.; Ruby, S. L.; Marks, T. J. *J. Am. Chem. Soc.* **1980**, *102*, 3322.
(17) (a) Burzynski, R.; Prasad, P.; Murthy, N. S. *J. Polym. Sci.: Polym. Phys. Ed.* **1986**, *24*, 133. (b) Murthy, N. S. *Macromolecules* **1987**, *20*, 309.
(18) (a) Tubino, R.; Piseri, L.; Carcano, G.; Pollini, I. *Solid State Commun.* **1980**, *34*, 173. (b) Mulazzi, E.; Pollini, I.; Piseri, L.; Tubino, R. *Phys. Rev. B* **1981**, *24*, 3555.
(19) Hardy, L. C.; Shriver, D. F. *J. Am. Chem. Soc.* **1986**, *108*, 2887.
(20) Nour, E. M.; Chen, L. H.; Laane, J. *J. Phys. Chem.* **1986**, *90*, 2841.
(21) Mizuno, M.; Tanaka, J.; Harada, I. *J. Phys. Chem.* **1981**, *85*, 1789.
(22) Sharp, S. B.; Gellene, G. I. *J. Phys. Chem. A*, **1997**, 101, 2192.
(23) Sperling, L. H. *Introduction to Physical Polymer Science*, Wiley: New York, 1992; Chapter 5.
(24) See Takemura, T. In *Progress in Polymer Science Japan;* Wiley: New York, 1974; Vol. 7, pp 224−272.
(25) Hirschfelder, J. O.; Curtiss, C. F.; Bird, R. B. *Molecular Theory of Gases and Liquids*; Wiley: New York, 1954; pp 25−30.

(26) Dallas, T.; Holtz, M.; Ahn, H.; Downer, M. C. *Phys. Rev. B* **1994**, *49*, 796.
(27) Piermarini, G. J.; Block, S.; Barnett, J. D.; Forman, R. A. *J. Appl. Phys.* **1975**, *46*, 2779.
(28) Ben-Amotz, D.; Herschbach, D. R. *J. Phys. Chem.* **1993**, *97*, 2295.
(29) Huheey, J. E.; Keiter, E. A.; Keiter, R. L. *Inorganic Chemistry: Principles of Structure and Reactivity*, *4*th ed.; Harper Collins: New York, 1993; pp 837−843.
(30) (a) Adams, D. M.; Ekejiuba, I. O. C. *J. Chem. Phys.* **1982**, *77*, 4793. (b) Adams, D. M.; Ekejiuba, I. O. C. *J. Chem. Phys.* **1983**, *78*, 5408.
(31) (a) Huang, Y.; Butler, I. S.; Gilson, D. F. *Inorg. Chem.* **1992**, *31*, 303. (b) Li, H.; Butler, I. S. *Inorg. Chem.* **1995**, *34*, 1193.
(32) Zheng, L. X.; Hess, B. C.; Benner, R. E.; Vardeny, Z. V.; Baker, G. L. *Phys. Rev. B* **1993**, *47*, 3070.
(33) See: Drickamer, H. G. *Acc. Chem. Res* **1986**, *19*, 329 and references therein.